Bulletin of the New Zealand Society for Earthquake Engineering, Vol. 58, No. 4, December 2025

STANDARDISED TIMBER MOMENT-RESISTING FRAMES FOR MULTISTOREY BUILDINGS: EXPERIMENTAL TESTING

Michael Newcombe[1*], Jack Tombleson[2], Sam Leslie[3] and Andrew Hewitt[4]

(Submitted *May 2024*; Reviewed *July 2024*; Accepted *March 2025*)

ABSTRACT

The paper presents experimental results and findings from several large-scale prototype moment-resisting timber frames. The overarching objective of this research was to provide standardised moment-resisting timber frame connections to support the increased application of timber in multistorey structures in NZ, akin to the 'Steel Connect' guide by SCNZ. The project was led by Red Stag Timberlab with support and funding by Callaghan Innovation. Enovate provided structural engineering design/detailing services for several prototype internal beam-column joint subassemblies, consulted on the experimental test set-up, apparatus, loading protocol and preliminary findings. Experimental testing on the sub-assemblies was performed by BRANZ.

The prototype sub-assemblies incorporated either Glue-laminated (Glulam) or Laminated Veneer Lumber (LVL) beams/column elements, and capacity-designed connections consisting of ductile steel plastic hinges/fuses designed to suppress brittle failure in the timber elements and provide energy dissipation/damping. This paper presents findings from the experimental testing to-date, highlights some critical design/detailing issues (identified through experimental testing), compares predicted versus observed frame flexibly, and makes recommendations for future design and research.

https://doi.org/10.5459/bnzsee.1696

INTRODUCTION

The application of engineered or mass timber frames as the primary gravity and/or seismic structural system in multistorey buildings is increasing throughout New Zealand and worldwide. A primary driver for this increased uptake is regulation or incentives to reduce embodied carbon in building projects/developments.

For commercial multistorey buildings, the required grid pattern/dimension between columns are typically between 8 to 9m. To resist just gravity loads for this size grid pattern, section sizes in glue-laminated timber (Glulam) or Laminated Veneer Lumber (LVL) become large and beam-column connection details can be challenging/complex; requiring careful consideration of anisotropic properties of timber (weakness perp-to-grain), char characteristics of the timber during fire, potential brittle failure modes of connections, aesthetics, acoustic flanking (as columns are often exposed) and creep. Add into the mix the requirement for the timber frame to provide resilient lateral resistance under seismic loading and the design challenge increases greatly. Designers are typically concerned by the lack of robust/comprehensive design guidance, lack of experimental testing and validation, the complexity of detailing (required to satisfy many performance/loading criteria), the inherent flexibility of moment-resisting timber connections, and the risks associated with an alternative solution (non-prescriptive) compliance pathway. For these reasons, many designers may be dissuaded from applying large timber moment frames for a project.

The structural engineers or researchers that have designed seismic-resistant large-scale moment-resisting timber connections (in New Zealand) have come up with a broad spectrum of details/solutions; none of which one would consider standard or broadly applicable. In the 1990's, Buchanan and Fairweather [1] designed and tested several beam-column joint details for Glulam frames (see Figure 1a), some of which exhibited brittle failure modes (see Figure 1b). This research and the connection details where subsequently referenced by the Timber Design Guide [2], but this did not lead to significant uptake by designers.

In 2005, research commenced at the University of Canterbury on post-tensioned timber frames (termed PresLam). This research [3-5] provided a novel approach for providing moment-resisting timber connections, which has been applied to several buildings within New Zealand (and overseas). However, challenges remain with complexity of the seismic design process and connection detailing, the potential for long-term creep induced post-tensioning loses, the requirement for specialist subcontractors during construction (for post-tensioning), complications for fire performance/design. Hence, the application of PresLam moment-frames since 2005 has been limited, when compared to growth of steel moment frames during the same period.

In 2020, NZ Wood provided some guidance on the seismic design of timber structures [6]) (including moment frames) and the design/detailing of post and beam timber construction [7]. These documents summarize the 'state-of-play' for timber moment frames in New Zealand. The only large-scale moment resisting timber frames cited/referenced utilize post-tensioned connections. Further, international publications on this topic are sparse [8].

[1] *Corresponding Author, Director, Enovate Consultants, Auckland, New Zealand, Email: michael.newcombe@enovate.co.nz*
[2] *Enovate Consultants, Auckland, New Zealand, Email: jack.tombleson@enovate.co.nz*
[3] *Red Stag Timberlab, Auckland, New Zealand, Email: sam.leslie@redstag.co.nz*
[4] *Red Stag Timberlab, Auckland, New Zealand, Email: andrew.hewitt@redstag.co.nz*

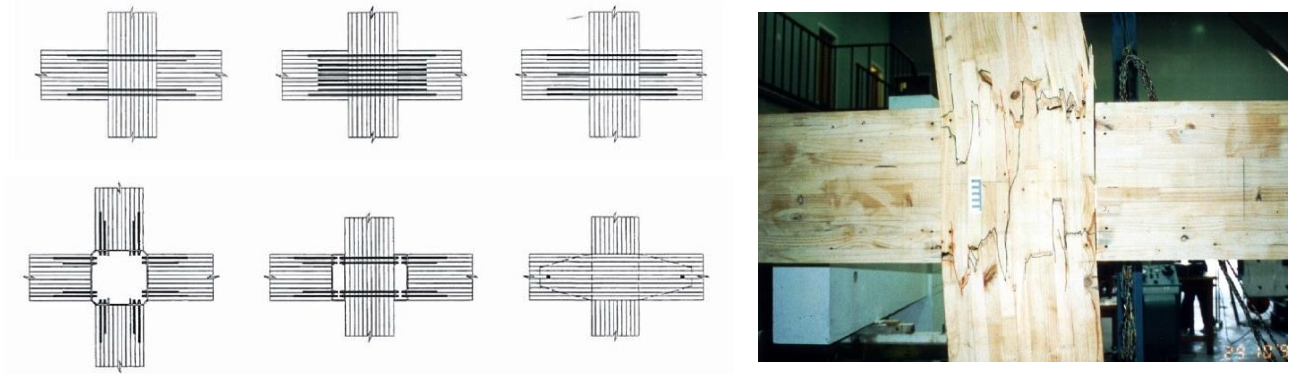

a) b)

Figure 1: Beam-column joint details tested by Buchanan and Fairweather [1]: a) Beam-column joint details, b) Brittle failure mode of continuous column with epoxied rods.

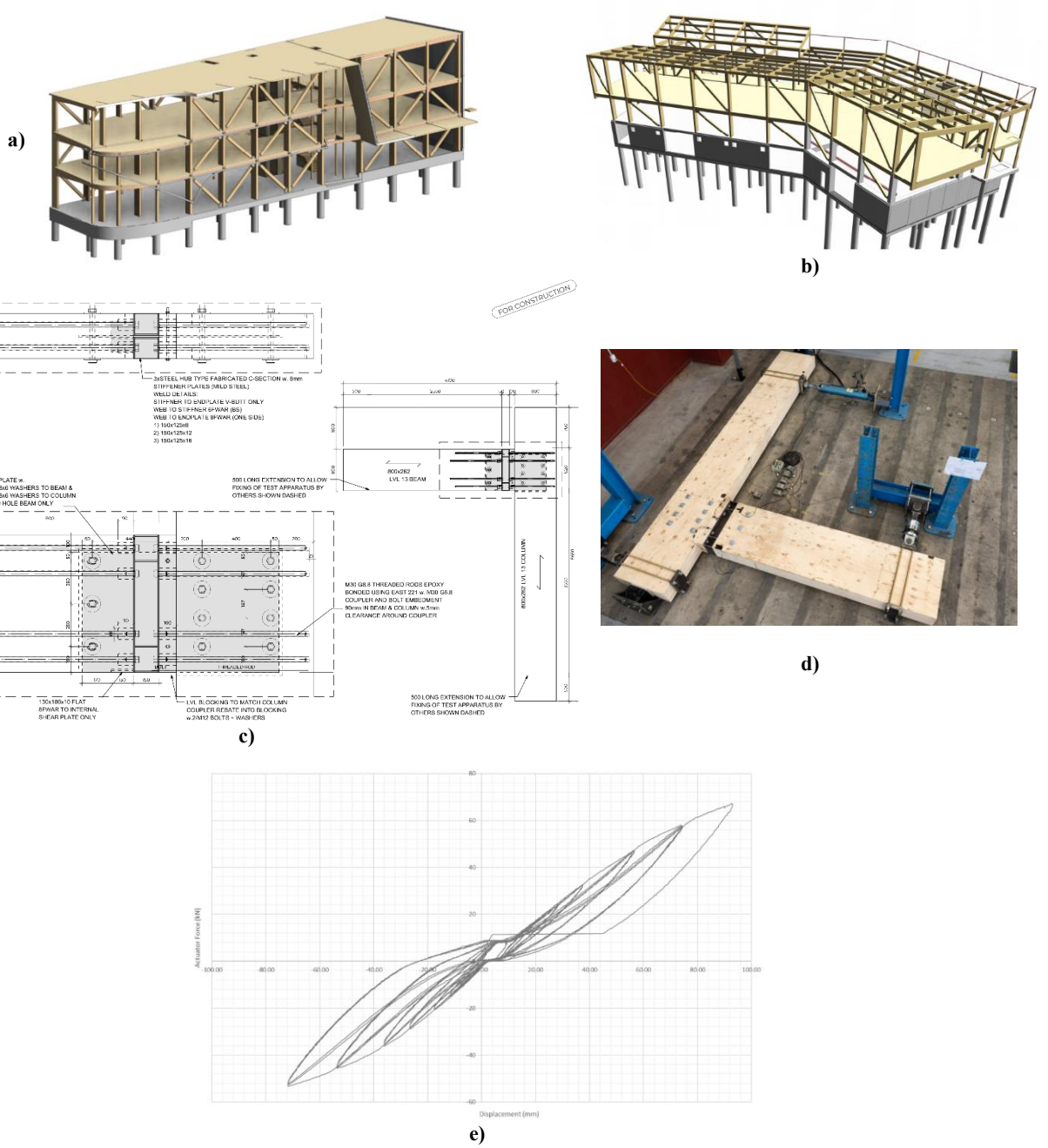

Figure 2: External beam-column joint hub connection: a) Arawa Street Project, b) Otago Polytechnic Trades Training Centre Project, c) Test specimen (c.o. Red Stag Timberlab), d) Test set-up, and e) Ram force versus displacement hysteresis loop.

Over the past eight years Enovate has developed large-scale ductile moment resisting timber frames that build on the research by Buchanan and Fairweather [1] and do not require post-tensioning. These connection details were developed for two projects Arawa Street (for Rotoma No. 1 Trust) and the Otago Polytechnical Trades Training Centre (He Toki Kai Te Rika), illustrated in Figure 2a and Figure 2b. Both projects incorporate a single bay moment frame with an overall span of 12 meters, with a spacing of 4.6 meters and 6 meters respectively.

It was recognised that experimental testing of the external beam-column connection detail (termed the "External Hub Connection") was required to validate the design. The detailing of the external beam-column subassembly is shown in Figure 2c. The prototype was manufactured by Red Stag Timberlab and was tested at Holmes Solution's Structural Testing Lab (see Figure 2d). The beam-column connection incorporates epoxied rods into the end of the beam section and through the width of the column, and a steel hub on the column face. The endplates of the steel hub were designed as a ductile fuse or potential ductile element using yield-line theory by Johnstone and Walpole [9]. The experimental results showed a minor degree of softening/yielding (see Figure 2e), providing low levels of energy dissipation. Connection slop and elastic deformations were larger than initially predicted, limiting the level of ductility that could be achieved during testing (with the connection slop resulting in some pinching). The test results did validate design assumptions for the project; achieving well over the design bending/shear demands (without a brittle failure) within allowable displacement/drift limitations. It was recognised that the future application External Hub Connection is limited due to experimental verification being limited to only external beam-column joints.

On these projects, a lot of design time was spent on connection design/detailing/verification due to a lack of guidance on standard/optimal large timber moment connections. The details are likely one-off/bespoke, are complex, costly and have heightened risk of failure (if sufficient experimental verification was not carried out). This appears to be a common theme for other engineers that have attempted to design/detail large-scale timber moment frames on other projects. Comparatively, the design and specification of moment resisting steel frames is straight forward by utilising the 'Steel Connect" guide by SCNZ [10]. Steel Connect includes a broad range of moment-resisting steelwork connections/details supported by detailed calculations and validated by experimental testing. Consequently, moment-resisting steel connections have become standardised, reducing cost/risk and increased market share of steel frame structures. The timber industry needs to follow this example to increase the uptake of large timber frame structures.

A key step in this direction began in 2021, when Red Stag Timberlab pursued and was granted funding through Callaghan Innovation to perform a R&D initiative termed "Project Skyscraper". Project Skyscraper aims to provide design/specification guidance for standardized moment-resisting timber connections (backed by experimental testing). Enovate were engaged to provide structural design/detailing of prototype internal beam-column connections/subassemblies, consult on the experimental testing, analyse test results, and assist with the development of a proprietary design/specification guide (for Red Stag Timberlab). The testing on beam-column joint subassemblies was performed by BRANZ at their Structural Testing Lab. This paper documents this research initiative, and is accompanied by a research report and a comprehensive design guide that was submitted to Red Stag Timberlab. The design guide is akin to SCNZ Structural Steel Connection Guide and can be sourced through Red Stag Timberlab.

PROTOTYPE TEST SPECIMENS

Three different types of internal beam-column joint subassemblies were designed and tested: a continuous column with steel beam-ends (termed *Continuous Column*), a spliced column with beam-end and column steel hubs (termed *Spliced Column*) and a continuous column with internal beam-end and column gussets (termed *Fish-Tail*). The connection details are illustrated in Figure 3.

Note: key connection details are omitted that are critical to the performance of the connection. This is partly to protect the intellectual property of Red Stag Timberlab but also to avoid replication of the detailing (without sufficient guidance). In the interim, applying similar details to projects is strongly discouraged without performing experimental testing and verification.

The design of prototype beam-column joints aimed to achieve the following key performance criteria:

1. Rapid on-site assembly. All three subassemblies allow for the beam-column connections to be quickly bolted together on site. All steel plates, dowels, epoxied rods are expected to be factory installed. This minimises on site labour cost and speeds up on-site assembly.
2. Incorporate a ductile fuse that is resilient, replaceable and allows for disassembly. All three subassemblies allow for ductile steel (potential ductile elements) that can be removed and replaced after an earthquake (reducing probable losses and repair time after a large earthquake). Replaceable connections also allow for disassembly, re-use/recycling of the structure (enhancing sustainability and reducing embodied carbon).
3. Steel components to be cost-effective and standard (without compromising 1 and 2). For the design of all subassemblies, standard universal steel sections (UB's) and bolts were used where possible to limit cost and supply lead-times. However, the structural requirements of the connection did require some bespoke welding/fabrication to achieve KPI 1 and 2 above.
4. Allow for fire protection/performance. The connection detailing must allow for fire protection options. Epoxied rod connections were not considered for shear transfer (to avoid a loss stability) and where possible steel components were detailed to sit within to beam/column section dimensions, allowing for timber covers or fire-rated linings to be applied over steel components.

For each type of beam-column joint, three sizes were designed/tested (large, medium and small). Table 1 summarizes all the tests/test specimen to-date. It is noted that the Continuous Column testing did not proceed beyond Test 3 for reasons cited in section 4. Only Glulam was used for the test specimen, except for Test 3 which used LVL. Glulam was considered worst-case for the risk of brittle failure in the timber sections (i.e. the material strength is lower, and section is less homogenous).

Perpendicular to grain reinforcement to prevent dowel-induced or shrinkage-induced splitting (along the grain) was not included in any test specimens (except Test 9). This reinforcement is required in practice but was conservatively not applied to the test specimens, thereby allowing any potential brittle failure modes to occur during testing.

Continuous Column (Test 1 and 3)

This first subassembly designed was the continuous column (see Figure 3a). Between the beams and the column is a structural steel hub; a short beam section with necked (or dog-boned) flanges. The necked flanges in the beam hub are

designed to be the potential ductile element within the system. The degree of necking is specifically tailored to maximise the strength and efficiency of the frame while ensuring that the timber elements and other components of the connection are capacity protected. The necking design/detailing follows Eurocode 8 [11], similar to the provisions from ANSI/AISC 358 [12] for reduced beam sections.

The hub is connected to the column and beam-end with a single row of two epoxied rods top and bottom to resist flexural actions. An internally slotted plate with mild steel dowels at the centre of the beam-end is provided to resist shear. The hub is bolted to couplers at the ends of the epoxied rods and tapped holes in the shear bracket which allows it to be removeable. An additional block of timber is provided on each side of the column to house the large couplers and shear bracket recess to prevent creating a large notch/void in the column at its edges.

The Test 3 specimen was designed after Test 1 was complete. The design of the Test 3 specimen attempted to avoid the column fracture observed during Test 1 (see the *Experimental Results* section) by using LVL and by increasing the column section size/modulus.

Spliced Column (Test 2, 4 and 5)

The second prototype subassembly designed was the Spliced Column (see Figure 3b). A short structural steel column section is used to splice the timber column together. Removeable beam hubs are used as the potential ductile element (like the Continuous Column). Three rows of two epoxied rods are provided to the column-ends. The outer rows are to resist flexural actions, while the middle row provides increased tension capacity and additional minor axis flexural strength (to avoid buckling). Two options for the column shear connection were explored. The first was applied to the medium specimen and incorporated slotted cleats with mild steel dowels. The second option incorporates bearing plates at the edge of the column and was applied on the large and small test specimen. The latter option is preferred as it is easily scalable for different column shear demands. The steel beam-column joint is designed to NZS3404 [13], using SCNZ connections [10] where possible. Note: for Test 2 the joint panel region was not reinforced with doubler plates to satisfy NZS3404 (see the *Experimental Results* section). This was not the case for Test 4 and 5.

Table 1: Test schedule.

Test No.	Type	Size	Material	Column size/grade	Beam size/grade
Test 1	Continuous Column	Medium	Glulam	990 x 230 GL10	900 x 230 GL10
Test 2	Spliced Column	Medium	Glulam	990 x 230 GL10	900x230 GL10
Test 3	Continuous Column	Medium	LVL	1000 x 343 LVL13	800 x 258 LVL11
Test 4	Spliced Column	Small	Glulam	720 x 230 GL10	630 x 230 GL10
Test 5	Spliced Column	Large	Glulam	1215 x 230 GL10	1125 x 230 GL10
Test 6	Fish Tail	Medium	Glulam	990 x 360 GL10	900 x 360 GL10
Test 7	Fish Tail	Large	Glulam	1215 x 360 GL10	1125 x 360 GL10
Test 8	Fish Tail	Small	Glulam	720 x 230 GL10	630 x 230 GL10
Test 9	Fish Tail	Large	Glulam	1215 x 360 GL10	1125 x 360 GL10

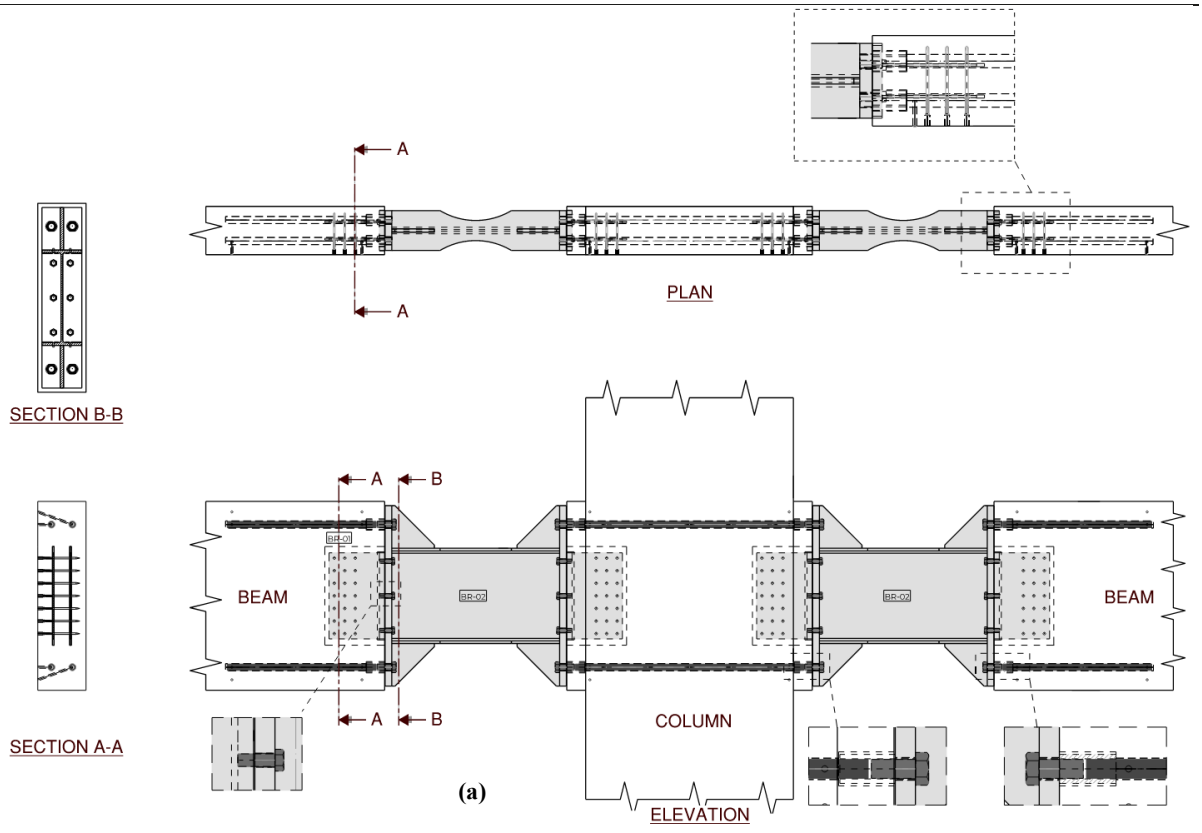

Figure 3(a): Red Stag Timberlab shop drawing models for the tested internal beam-to-continuous column joint.

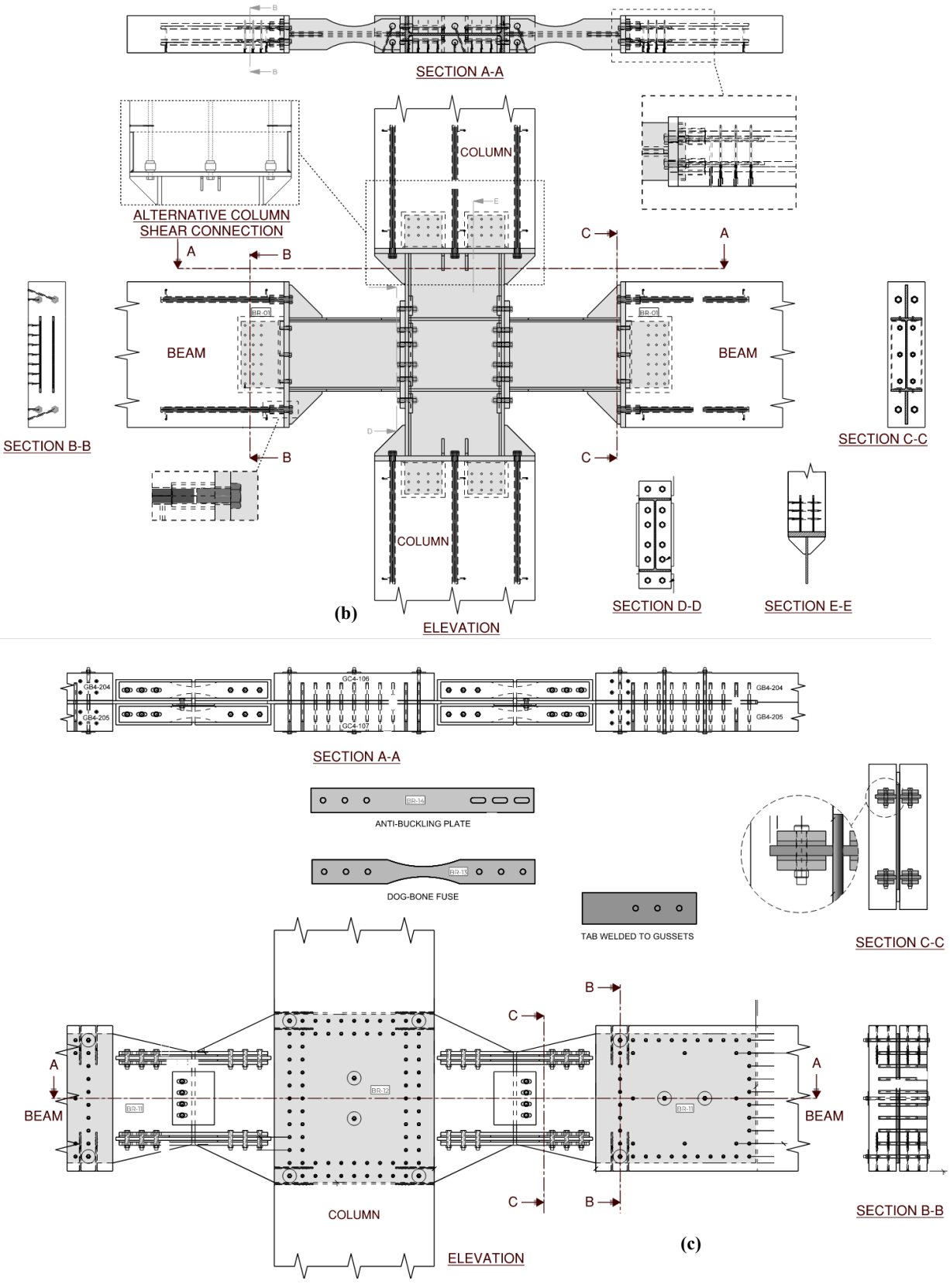

Figure 3: Red Stag Timberlab shop drawing models for three types of internal beam-column joint details tested (under Project Skyscraper): a) Continuous Column, b) Spliced Column, c) Fish-Tail.

Fish Tail (Test 6, 7, 8 and 9)

The third prototype subassembly was the Fish Tail (see Figure 3c). This prototype gets its name from shape made by the column and beam gussets. The column is intended to be made in two pieces and block-glued around the column gusset plate to avoid welding of gusset tabs plates near the timber column. The column and beam-end gusset plates are fixed in place using mild steel dowels arranged around the perimeter of the gusset and bolted towards to the centre of the gusset. The bolts provide clamping in the minor axis direction of the beam and column, preventing splitting.

The column and the beam-end gussets are connected to potential ductile elements/fuses at the top/bottom of the beam to resist flexural action and bolts (in slotted holes) at the centre to resist shear. The fuses for the prototype design are necked/dog-bone shaped mild steel plates, designed to yielding in tension and compression. Clamping/anti-buckling plates are provided each side of the fuses to prevent buckling under compressive loads. The clamping plates are slotted on one side to avoid contribution to the flexural strength of the connection. Note: it is intended that any ductile fuse could be used within this connection arrangement including friction-slip plates or Tectonus devices or similar.

The mild steel dowels around the perimeter of the gussets are capacity designed elements and resist moment/shear and axial forces using a Rivet Group Analogy based on equations from the Timber Design Guide [2]. Splitting reinforcement screws are provided to the ends of the beam to prevent splitting in accordance with recent recommendations [14].

After analysis of the Test 6 results, it was identified that the slop in the bolted connections for the dog-bone steel plates significantly contributed to the flexibility of the subassembly (see the *Experimental Results* section). Hence, for Test 7 and 8, the dog-bone plates were welded in place to the gusset tabs.

Test 9 was a repeat of Test 7 and aimed to eliminate some of issues/errors in the test set-up/loading protocol noted in section 3 and to qualify additional sources of flexural strength within the beam-column connection.

TEST SETUP AND LOADING PROTOCOL

Quasi-static loading was applied to the internal beam-column joint subassembly at the top of the column in accordance with the ACI 374.2R-13 [15] displacement protocol (see Figure 4a and Figure 4b). Potentiometers were placed around the steel to timber interfaces to allow assessment of connection slop (see Figure 4c), over the ductile fuses and at all reaction points.

Some issues/errors in the test set-up/loading protocol that affected some test results are listed below:

- The distance between column/beam reactions did not match the initial prototype design. The distance between column reactions was 4.8m (not 4.0m as designed) for Test 4, 5 and 6, and the distance between beam reactions for Test 4 was 8m (not 6m as designed for the small prototype specimens). While this did not affect the validity of the experimental response/data, initial predictions of the yield displacements (used for the loading protocol) were underestimated.
- There were two beam reaction frame failures for Test 7. Firstly, the steel components providing the tensile beam reaction failed, then the column-base lateral restraint failed. These failures potentially had a minor effect on the small cycle test data (that indicates the initial stiffness) but this is assessed in section 4.
- Test 9A (a repeat of Test 7) and 9B reached the maximum capacity of the loading apparatus and had to stop prior to the completion of the loading protocol. See the *Experimental Results* section for more detail.

EXPERIMENTAL RESULTS

Key experimental observations are summarized in Table 2 and in Figure 5. The hysteretic response for Tests 1 to 8 is shown in Figure 6 and Figure 7. The primary axes are column moment (at the centreline of the beam) versus column drift (between column restraints). The secondary axis gives the ram force versus ram displacement at the top of the column.

All experimental results are compared against analytic predictions for the yield force/moment and displacement/drift as described in the *Predicted Frame Strength/Stiffness* section.

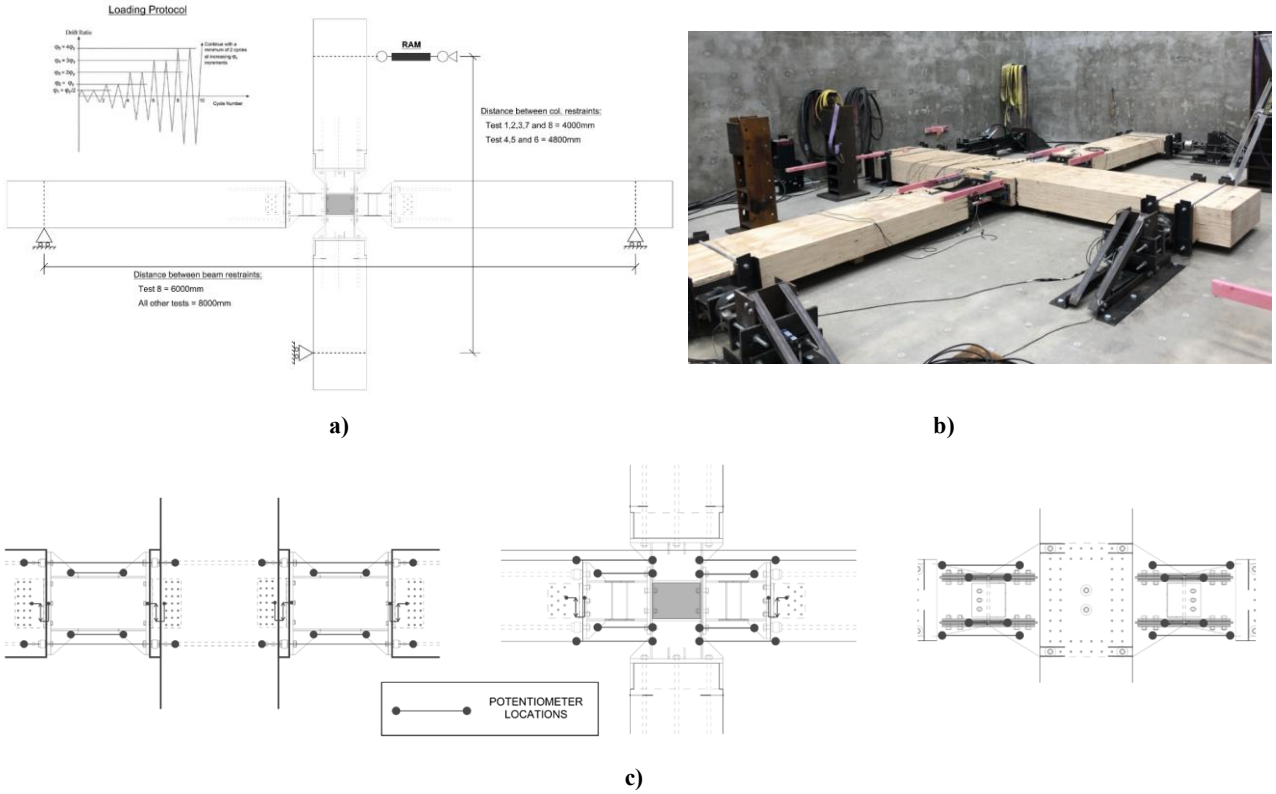

Figure 4: Test set-up and loading protocol: a) Loading protocol and beam/column reaction points, b) Image of test setup, c) Beam-column joint potentiometers.

Table 2: Experimental observations.

Test No.	Type/Size	Key Observations
Test 1	Continuous Column/ Medium	Test 1 exhibited essentially linear-elastic response until a sudden brittle failure/fracture of the column occurred (just above the predicted yield force/moment). The failure appeared to be in a flexural mode, but the flexural demands on the column were well within the design flexural capacity. See Figure 5a, where the fracture is highlighted. See the *Continuous Column Failure* section where this failure is discussed further.
Test 2	Spliced Column/ Medium	Test 2 exhibited a non-linear Ramberg-Osgood style hysteresis (typical for ductile steel structures), but with a high portion of elastic deformation. During the first cycle beyond 3% drift, the dog-boned flange of the beam hub exhibited lateral torsional buckling (see Figure 5b). Yielding of the joint panel region was observed below the predicted yield force due to the lack of double plates (required by NZS3404 but omitted for the design of the specimen). This is expected to have increased the ductility and hysteretic damping of the test.
Test 3	Continuous Column/ Medium	Test 3 began to exhibit non-linear behaviour at low levels of ductility, then quickly began to lose strength as the column exhibited a brittle failure in a similar manner to Test 1 (see Figure 5c).
Test 4	Spliced Column/ Small	Test 4 exhibited a similar response to Test 2, but with less hysteretic area/damping (potentially because the joint panel region did not yield at low force/displacement like Test 2). The level of ductility achieved during the test was limited due to the distance between beam reactions being greater than intended (see the *Test Setup and Loading Protocol* section). Note: the predicted yield force/displacement was updated to allow the actual/tested distance between column reactions.
Test 5	Spliced Column/ Large	Test 5 exhibited a similar response to Test 4, but ductility was limited due to increased flexibility of the frame (see the *Spliced Column* section) as well as the incorrect column reaction distance being used (see the *Test Setup and Loading Protocol* section). The predicted yield displacement appears to be underestimated when compared to the test data. Refer to the *Spliced Column* section for more information.
Test 6	Fish Tail/ Medium	The hysteretic response for Test 6 was pinched but appeared to have a high friction component (resulting in high hysteretic damping/area). The pinching was primarily due slop in the bolted connections for the dog-bone fuse plates. Slop could be easily eliminated by modifying the fixing details of the dog-bone fuse to the gusset tab such as using friction-slip or other proprietary devises. The friction component was potentially generated by the anti-buckling plates, observed to undergo minor axis bending during the testing (see Figure 5d). Further, the minor axis bending on the anti-buckling plates and dog-bone fuses are expected to have contributed to the flexural capacity of the test specimen. The dog-bone plates did appear to yield in tension and compression at large drifts as indicated in Figure 5e.
Test 7	Fish Tail/ Large	The Test 7 hysteresis exhibited less pinching than Test 6 as the dog-bone plates were welded to the gusset tabs. However, the dowels around the perimeter of the gussets contribute to some hysteretic pinching. Due to experimental issues/errors (see the *Test Setup and Loading Protocol* section), the initial stiffness is expected to be underrepresented in the positive quadrant. Similar to Test 6, the flexural capacity was higher than predicted
Test 8	Fish Tail/ Small	The Test 8 hysteresis exhibited low levels of pinching and high levels of energy dissipation/damping. Displacement cycles proceeded to an approximate ductility of 4 (or a drift of 4.5%), when dog-bone plates fractured due to low-cycle fatigue. Some vertical column splitting did occur at the corner of the column dowel pattern (see Figure 5f) indicating that some transverse reinforcement may be required.
Test 9A, Test 9B Test 9C	Fish Tail/ Large	Test 9A was a repeat of Test 7 and reached the maximum capacity of the loading apparatus a lateral displacement of 90mm or 2.2% drift, resulting in termination of the test. Note: before Test 9A was terminated five additional displacement cycles were applied with peak lateral displacements between 81mm and 90mm, which subjected the dog-bone fuses to a higher number of inelastic cycles (than required by the loading protocol). The test specimen was unloaded to 0mm displacement (at the top of the column) and the inner four dog bones were cut to reduce the lateral strength of the test specimen (see Figure 5h). Testing recommenced (Test 9B) from the beginning of the 81mm displacement cycle. Again, the maximum capacity of the loading apparatus was reached at 135mm or 3.3% drift. The test specimen was unloaded, and the inner four anti-buckling plates were cut to further reduce the strength of the test specimen. Testing recommenced (Test 9C) from the beginning of the 81mm displacement cycle. During the first 108mm displacement cycle (2.7% drift) one of the dog-bone fuse fractured due to low-cycle fatigue (see Figure 5i). Testing continued until the 162mm displacement cycle (4.0% drift) one dog-bone fuse on both the top/bottom of the beam had fractured (see Figure 5j). The hysteretic response for Test 9A was similar to Test 7, except the strength and initial stiffness in the positive quadrant for Test 9A was significantly higher than Test 7. This supports the assertion that experimental issues/errors effected that experimental response in the positive quadrant in Test 7. During large displacement cycles the minor axis bending of the dog-bone fuses and associated anti-buckling plates could be observed (see Figure 5j). Comparison of the hysteretic response for Test 9A, 9B and 9C enables approximation of the flexural contribution due the minor axis bending and axial resistance of the dog-bone fuses and anti-buckling plates. Refer to the *Quantification of Capacity Components for the Fish Tail Connection* section for more information.

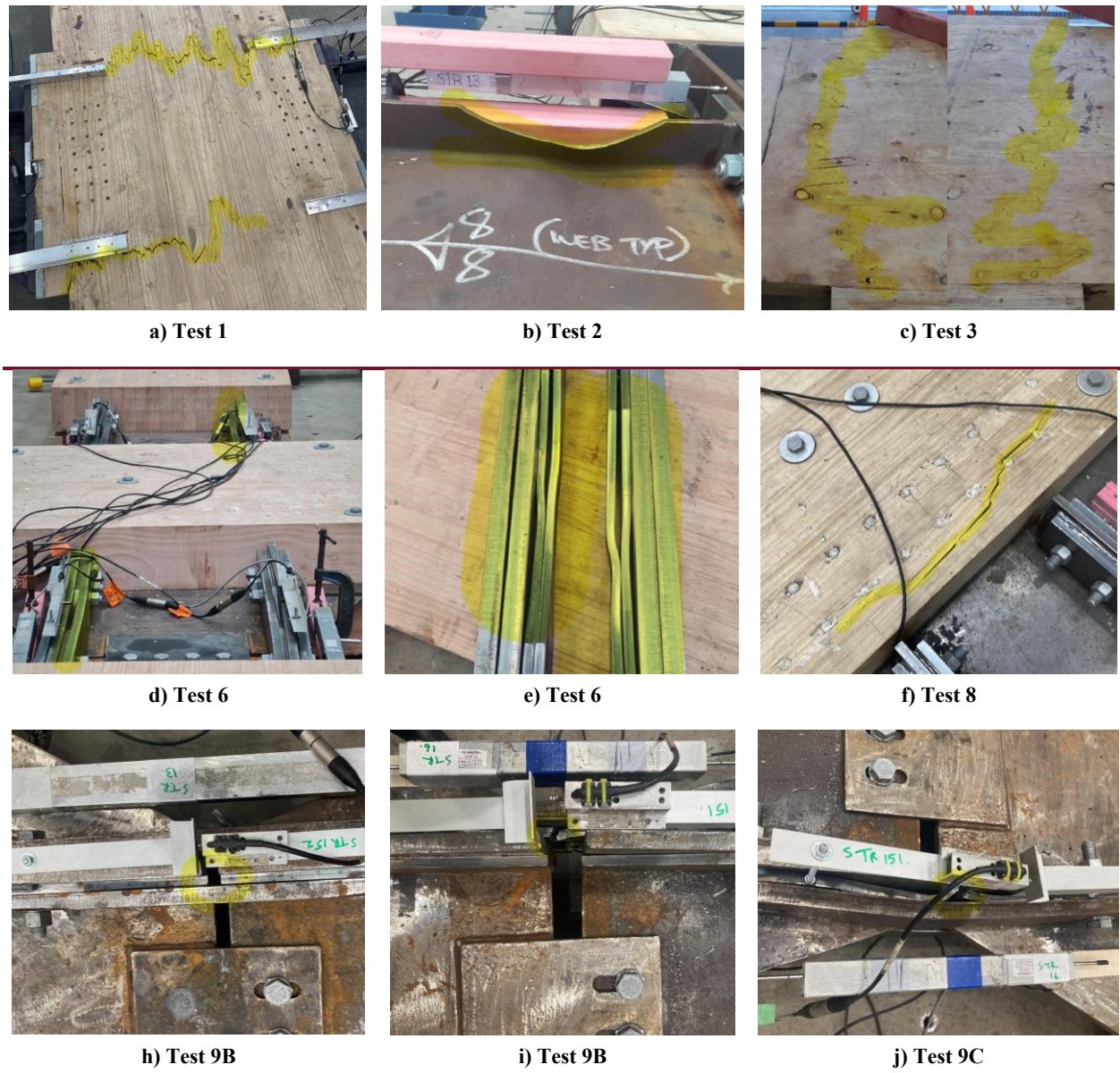

a) Test 1 b) Test 2 c) Test 3

d) Test 6 e) Test 6 f) Test 8

h) Test 9B i) Test 9B j) Test 9C

Figure 5: Key experimental observations for Tests 1, 2, 4, 6, 8, 9A, 9B and 9C.

EXPERIMENTAL ANALYSIS

In this section, key aspects of the experimental results are analysed including the predicted versus actual frame strength and stiffness (at and to the yield point), the brittle failure of the Continuous Column test specimen, the lateral buckling of the dog-boned flanges in the beam hubs, the requirement for column reinforcing screws for the Fish Tail connection and the quantification of additional sources of strength for the Fish Tail Connection.

Predicted Frame Strength/Stiffness

The strength and stiffness of each frame was predicted at and to the yield point.

The yield strength of the frame (represented as column moment in Figure 6 and Figure 7) for the Continuous and Spliced Column connection was determined considering the yield moment (yield stress multiplied by the plastic section modulus) of the reduced beam sections with dog-bone flanges, then projecting the yield moment at the connection to the centreline of the column. The yield stress of the dog-bone flange was taken at 10% greater than the published characteristic value from the supplier (330MPa).

For the Fish Tail connection, a similar procedure was applied but the yield moment of connection was determined considering the yield axial force of the dog-bone fuses and multiplying by the lever arm between the dog-bone fuses. The yield stress of the steel as per the mill certificates for the dog-bone fuses was considered (353MPa).

Analytical equations by Newcombe (2012) were used as the basis for prediction of the yield drift for each test specimen. For each type of subassembly, different assumptions were made to predict contribution of the drift components described in Equation 1:

$$\theta = \theta_b + \theta_c + \theta_j + \theta_{con} \quad (1)$$

where θ_b= the flexural and shear deformation of the beams; θ_c= the flexural and shear deformation of the columns; θ_j= the shear deformation of the joint panel region and θ_{con} = the beam-column connection. For the three connection types, these drift components are treated as summarized in Table 3.

For brevity, the design procedures for the prediction of frame strength and stiffness and recommended structural modelling approaches will be covered in more detail in future publications.

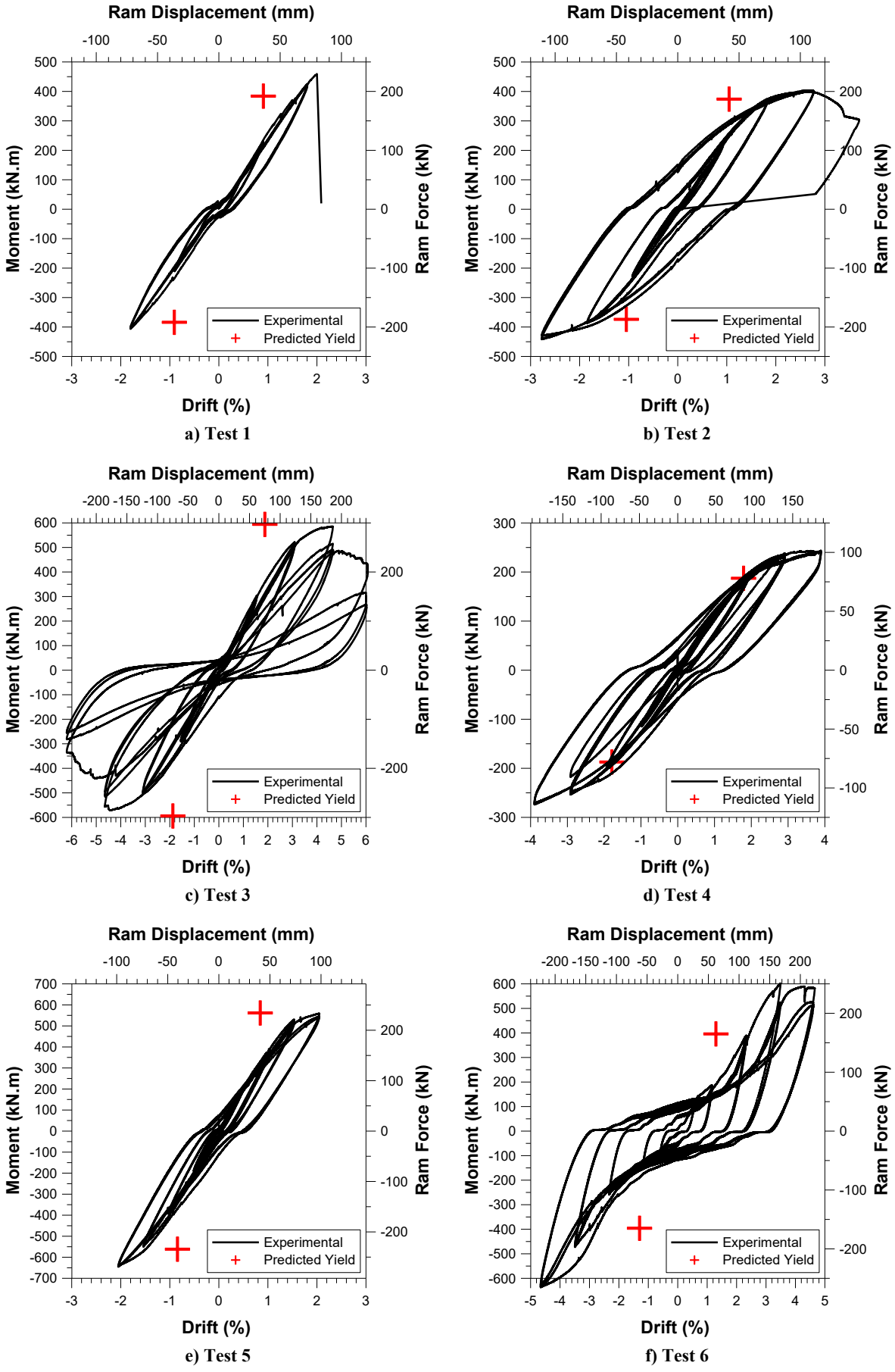

Figure 6: Lateral ram force versus displacement hysteresis plots for Test 1 to 6.

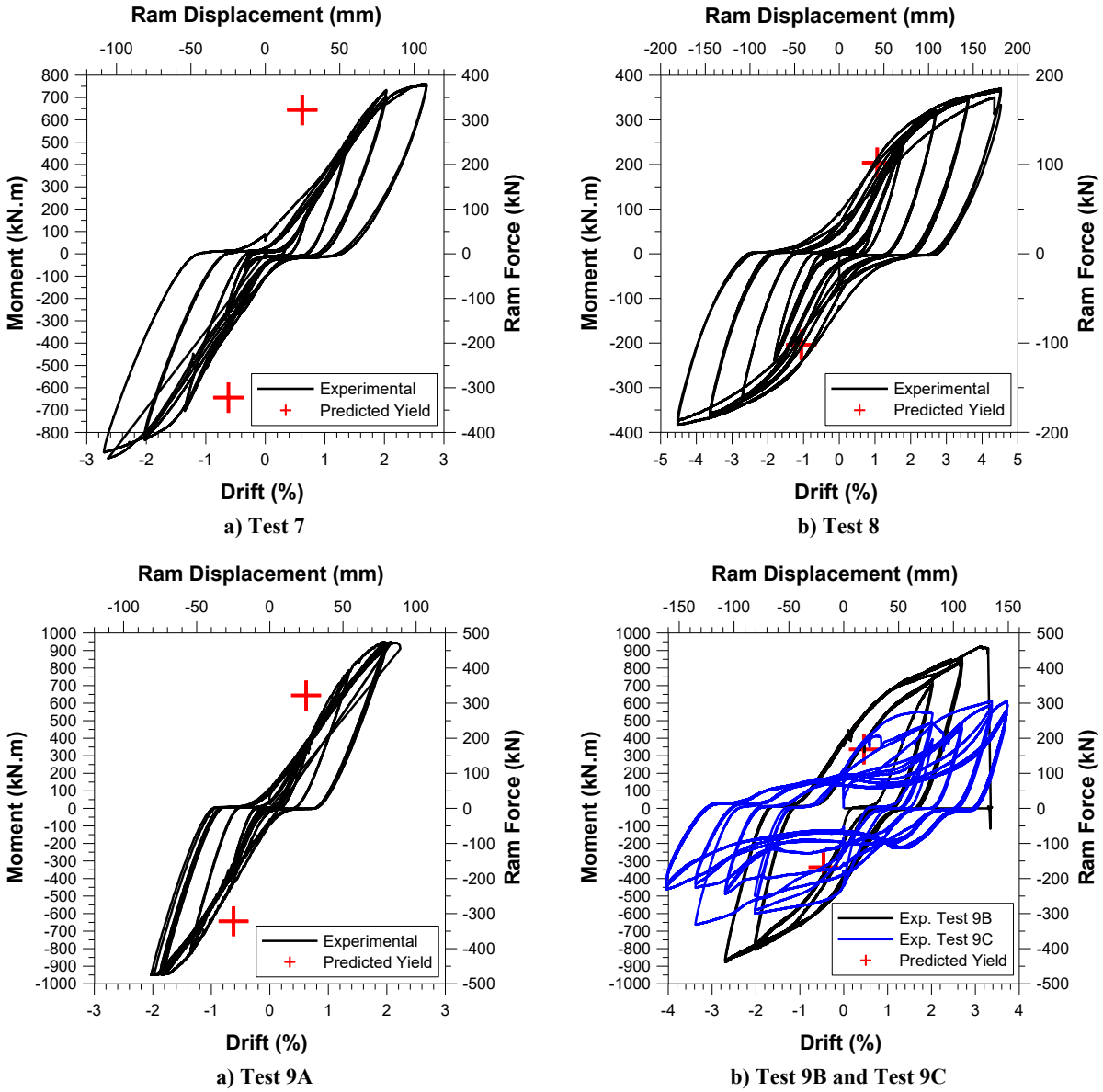

Figure 7: Hysteresis plots for Test 6 to 8, Test 9A, and Test 9B & 9C.

Table 3: Frame flexibility assumptions.

Connection Type	Drift Component Assumptions		
	$\theta_b + \theta_c$	θ_j	θ_{con}
Continuous Column	Included	Included. Refer Newcombe [5].	Sum of 1mm slop/strain penetration assumed for all epoxy rods in tension or compression
Spliced Column	Included	Ignored (determined to be insignificant)	Sum of 1mm slop/strain penetration assumed for all epoxy rods in tension or compression
Fish Tail	Included	Ignored (determined to be insignificant due to gusset plate)	Dowel deformation (to EC5 equations) of column/beam-end dowel patterns combined and dog-bone plate bolted connection slop (where applicable).

Continuous Column (Test 1 and 3)

The predicted frame stiffness is too high relative to the experimental results. This could potentially be due to significant strain penetration of the epoxied rods in the column section that is not accounted for in the analytical equations (i.e. greater than 1mm per rod). This is supported by review of potentiometer data (at the connection interface) which indicates up to 2.5mm of slop/strain penetration per rod.

The predicted yield force/moment appears to be relatively accurate but premature column fracture does limit a more accurate assessment.

Spliced Column (Test 2, 4 and 5)

The predicted frame stiffness is considered accurate for Test 2 and 4. However, for Test 5 the predicted frame stiffness is too high. Preliminary investigation of experimental data indicates that connection deformation on the right beam-end to column connection was higher than the left beam-end connection, indicating a potential anomaly in the beam/column fixings or support restraints. Deformation of the support restraints appears more likely, as this was evident for the large Fish Tail test (as described in the next section). On review of the test data, 7mm of lateral column deformation could be attributed to the movement of the steel reaction frame relative to the strong floor, and additional flexibility is expected where the steel reaction frame is connected to the column/beam ends.

The predicted yield force/moment appears to be relatively accurate for Test 4. The Test 2 prediction appeared to overestimate the yield force/moment as yielding of the joint panel was not considered. Test 5 was terminated too early to give a clear indication of the post-yield response.

Fish Tail (Test 6, 7, 8 and 9A)

The predicted frame stiffness is too high for Test 6, 7 and 9A, but is accurate for Test 8.

For Test 6, this can a partially explained by slop the bolted connections at either end of the dog-bone fuses. The predicted yield drift assumed slop in these bolted connections of only 1mm per dog-bone fuse end. However, review the experimental data indicates that the slop of the dog-bone fuse end connections (including bolt bearing deformation) was in the order of 3 to 4 times higher than predicted (3mm to 4mm per end). By contrast, the deformation of the welded dob-bone fuse ends from Test 9A was assessed to be less than 0.5mm.

The predicted frame stiffness for Test 9A is more accurate than Test 7 for reasons already stated earlier in the *Results* section. Yet, for Test 9A the predicted frame stiffness is too high (in the order of 50%), while Test 8 appears to be accurate. There are several explanations for the over predication of the stiffness for Test 9A, but most likely is that there are additional sources for flexibility associated with the support restraints (see Figure 4b) that are more significant for Test 9A compared to Test 8.

The restraints at either the ends of the beam/column sections rely on perpendicular-to-grain bearing and steel rods in tension, both relatively flexible mechanisms. Unfortunately, the test apparatus did not capture this component of frame flexibility and only measured the slip of the steel reaction frame to the strong floor. However, at the predicted yield force/moment, the elongation of the tension rods and bearing deformation was calculated to contribute approximately 5mm to the lateral displacement of the frame (at the predicted yield force). Further, the test data indicates that the column-base steel reaction frame moved by +/-4mm relative to concrete strong floor. This additional source of deformation accounts for near all the difference between the predicted and measured frame stiffness. Based on this and the accurate prediction of frame stiffness for Test 8, the analytical predictions for the frame stiffness are considered accurate.

The predicted yield force/moment appears to be low for all tests. Therefore, it is anticipated that there are other contributions to the bending strength of the beam to column gusset connections that has not been accounted for. This is likely to be due to the minor axis bending of the fuse and anti-buckling plates resulting in induced friction forces. This is considered further in the *Quantification of Capacity Components for the Fish Tail Connection* section.

Continuous Column Failure

Tests 1 and 3 both experienced a brittle failure of the column. The failure appeared to be a tensile failure of the Glulam or LVL parallel to grain that propagated from the ends of epoxied rods in the column. This failure mechanism appears to be similar to that exhibited during testing by Buchanan and Fairweather [1] shown in Figure 1 (but not investigated further).

After Test 1, a finite element analysis (FEM) of the column section was undertaken to identify why this may have occurred. Two thin-shell column FEM models were created using ETABS termed 'Benchmark' and 'Representative.' Both models considered the orthotropic properties for the tested Glulam/LVL.

The benchmark model applied the lateral load to the top of the column and provided pinned supports to all nodes in line with the centreline of beam. This model was used to represent the vertical column stresses that would be expected using simple beam theory and ignoring any disturbed stress states/regions around the epoxied rods. The resultant vertical stresses for the benchmark model are given in Figure 8a; the peak tension stress is 16.1MPa.

The representative model applied the lateral load to the top of the column and included the forces from the epoxied rods distributing into the column section. This model was used to represent vertical stresses induced in the column section due to both flexural demand and local stresses induced by the development of the epoxied rods in the column. The resultant vertical stresses for the representative model are given in Figure 8b; the peak tension stress is 41.1MPa.

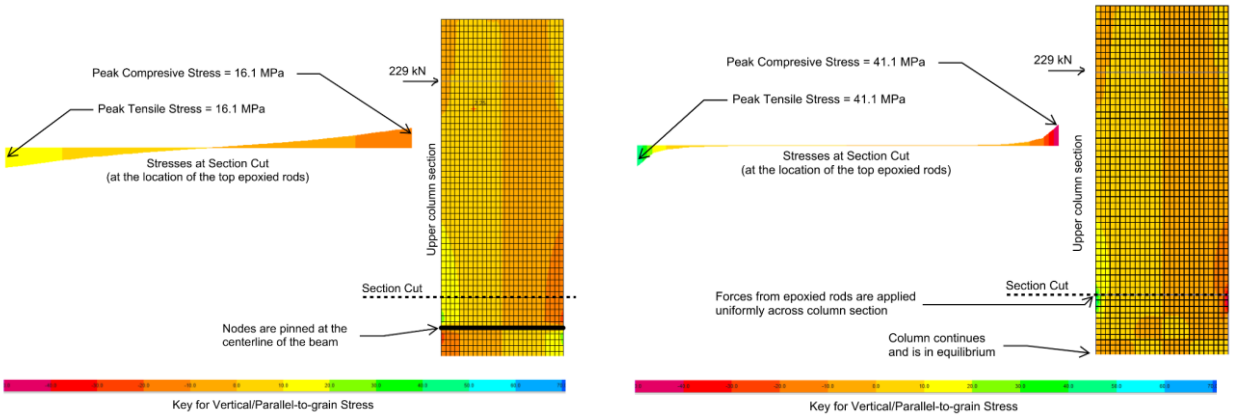

Figure 8: FEM analysis of Test 1 at failure: a) Benchmark model, b) Representative model.

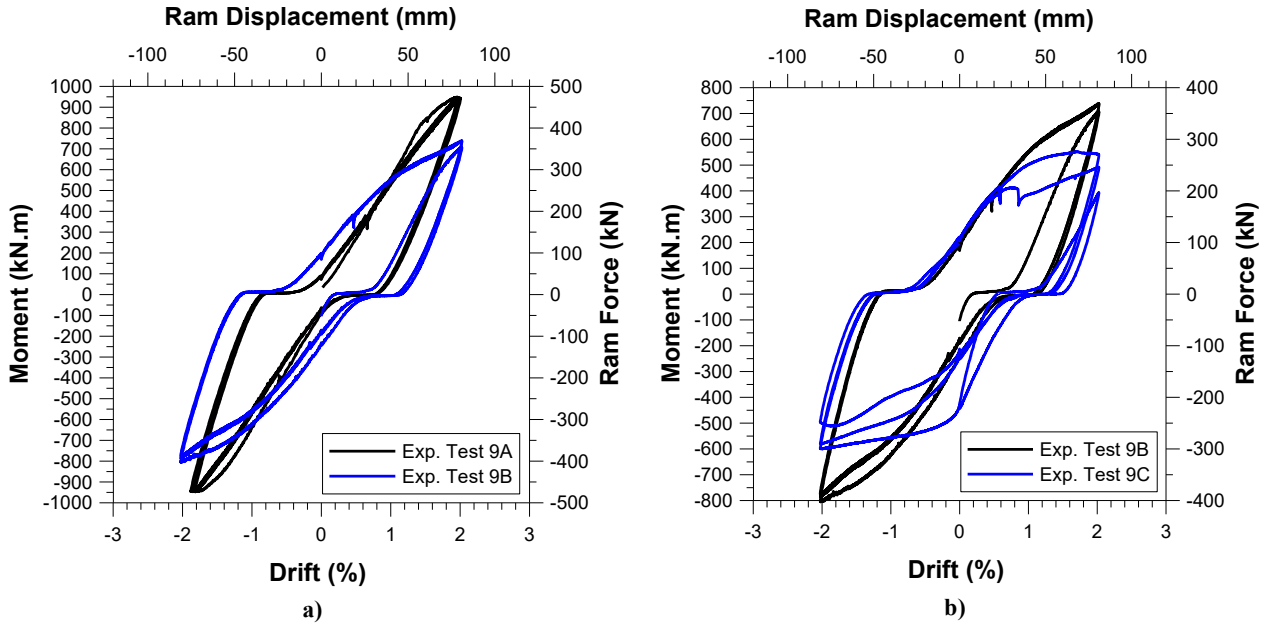

Figure 9: Hysteresis plot comparison for Test 9A versus Test 9B, and Test 9B versus Test 9C.

Comparison of benchmark and representative FEM results demonstrates that the vertical stresses in the column are greatly increased due to the 'bursting stresses' induced by the epoxied rods (by a factor of 2.5 in this case). This may be due to the low strength/stiffness of perpendicular to grain timber (that requires effective confinement from the parallel to grain timber to resist the bursting stresses). The peak stress of 41.1 MPa is far in exceedance of the characteristic bending strength of GL10 (22 MPa). *Caution is advised to designers that might be using similar details*.

Beam Hub Lateral Torsional Buckling

Test 2 resulted in a lateral torsional buckling in the dog-boned flange of the beam hub (see Figure 5b). This was despite the dog-bone details complying with EC8 [11]. Further, SCNZ have published guidance on the use of reduced beam sections in steel frames [16] and highlights that strength is gradually lost due to buckling of the reduced beam section but no advice on how to mitigate this issue. On further review, ANSI/AISC 358 [12] does require lateral (fly) bracing on either side of dog-boned flange and is recommended as best-practice moving forward.

For tests 4 and 5, two full depth flange stiffeners were positioned at third points within the reduced beam section to provide some degree of restraint to the critical flange (as fly braces could not be readily installed) and buckling of the dog-boned beam section was not observed.

Column Screw Reinforcing for the Fish Tail Connection

Tests 6, 7 and 8 were performed without screw reinforcement at the corner of the column dowel pattern. This was in accordance with recent design guidance on reinforcing timber members [14], which indicates the screw reinforcement is only required at the ends of timber members. However, Test 8 exhibited splitting along the length of the continuous column adjacent to the corner of dowel pattern (see Figure 5f). To suppress this brittle failure mode, its recommended that column splitting screws are also provided in accordance with Moroder and Smith [14] for future applications of the Fish Tail connection.

Quantification of Capacity Components for the Fish Tail Connection

Comparison of Tests 9A, 9B and 9C enables the evaluation of capacity components, including some components that were not accounted for in the predicted yield capacity. The hysteretic plots for Test 9A are compared with Test 9B and Test 9C for the 81mm lateral displacement cycle in Figure 9. The 81mm displacement cycle is selected as this cycle is common to all three tests and is prior any low-cycle fatigue failure of the dog-bone fuses.

Comparing Test 9A and 9B, the difference between the peak moment capacity (averaging the positive and negative values) is approximately 180kN.m. Based on analytical predictions of the internal dog-bone fuses flexural capacity, the difference in moment capacity (between Test 9A and 9B) should be in the order of 310kN.m. However, Test 9A has a higher proportion of elastic deformation when compared to Test 9B (of approximately 9mm) due to the higher actions in the frame and when this is accounted for the predicted internal dog-bone fuses flexural capacity aligns with the experimental data.

Comparing Test 9B and 9C, the difference between the peak moment capacity (averaging the positive and negative values) is approximately 200kN.m. Note: if the difference in elastic deformation between Test 9B and 9C was accounted for the difference in peak moment could be even greater. This difference in the peak moment indicates that the internal anti-buckling plates are contributing this capacity via a combination of minor axis bending and axial restraint via friction. The minor axis bending capacity of the internal anti-buckling plates is calculated to be only 16kN.m (projected to the max. column moment), indicating that axial resistance of the internal anti-buckling plates (at the connection) is at least 230kN. Therefore, the contribution of the anti-buckling plates to the capacity test specimen is significant and could result in a violation of the capacity design hierarchy. Therefore, future permutations of the Fish Tail connection should avoid this arrangement for the potential ductile element (PDE) to better control the overstrength of the frame. Refer to the accompanying design guide from Red Stag Timberlab for more information.

CONCLUSIONS

Experimental testing and analysis of several large-scale prototype moment-resisting timber frames has been presented. Three types of beam-column connections were designed and tested with varied results.

The Continuous Column Prototype (with epoxied rods through the width of the column) exhibited an unexpected brittle failure in the column joint panel region. This failure is expected to be due to bursting stresses created by the epoxied rods into the column, combining with flexural stresses. Caution is advised to any designers considering or specifying similar connection details.

The Spliced Column Prototype exhibited a stable and ductile seismic response and suppressed any brittle failure in the timber sections. However, suggestions are made for the detailing of the necked flanges on the beam hubs, to limit lateral torsional buckling.

The Fish Tail Prototype exhibited a stable and ductile seismic response. Minor modifications to the original design were required during the testing programme to limit connection slop in the system and to reinforce the column section (at the corner of column dowel pattern).

Analytical predictions for the frame stiffness (at the yield point) for the Spliced Column and Fish Tail prototype were validated. For the Spliced Column, the predicted yield strength was accurate. For the Fish Tail, the predicted yield capacity was underestimated due to the minor axis bending and axial restraint (via friction) from the fuses and anti-buckling plates (that was not accounted for in the prediction). For future designs of the Fish Tail, it is recommended that potential ductile elements (PDEs) between the column and beam gusset plates should be designed to limit overstrength (and thereby avoid additional sources of capacity that are not easily quantified such as minor axis bending and friction).

FURTHER RESEARCH

This research represents a significant contribution to the standardisation of large-scale moment resisting timber frames in New Zealand but further research is needed.

The flexibility of the Fish Tail Prototype is a significant advantage. Different plug-and-play potential ductile elements fixed to the beam/column gusset tabs (such as friction-slip or Tectonus devices) can be readily applied but noting that it is important to limit the overstrength of the system. Future small-scale testing/investigation on suitable potential ductile elements between gusset tabs is recommended.

ACKNOWLEDGMENTS

This is an updated and extended version of a paper presented at the NZSEE Annual Conference in Auckland in April 2024 [17]. The conference paper received high praise from the reviewer and was recommended for publication in the Bulletin. Since then, the paper has been further developed and has undergone additional independent review in accordance with the Bulletin's review policy.

REFERENCES

1 Buchanan AH and Fairweather RH (1993). "Seismic design of glulam structures". *Bulletin of the New Zealand Society for Earthquake Engineering*, **26**(4): 415-436.

2 Buchanan AH (2007). *Timber Design Guide*. New Zealand Timber Industry Federation, Wellington, NZ.

3 Palermo A, Pampanin S, Buchanan A and Newcombe M (2005). "Seismic design of multi-storey buildings using laminated veneer lumber (LVL)". *New Zealand Society for Earthquake Engineering Annual Conference*, 8pp.

4 Buchanan A, Deam B, Fragiacomo M, Pampanin S and Palermo A (2008). "Multi-storey prestressed timber buildings in New Zealand". *Structural Engineering International*, **18**(2).

5 Newcombe MP (2012). "*Seismic Design of Post-Tensioned Timber Frame and Wall Buildings*". PhD Dissertation, University of Canterbury, Christchurch.

6 Smith T (2020). "*Seismic Design*". Chapter 11.5 in *NZ Wood Design Guide*, Page 1-40. https://www.wpma.org.nz/timber-design-guides.html

7 Oliver L and White B (2020). "*Post and Beam Timber Construction*". Chapter 9.5 in *NZ Wood Design Guide*, Page 1-62. https://www.wpma.org.nz/timber-design-guides.html

8 Rebouças AS, Mehdipour Z, Branco JM and Lourenço PB (2022). "Ductile moment-resisting timber connections: A review". *Buildings*, **12**(2): 240.

9 Johnstone ND and Walpole WR (1982). "Behaviour of steel beam-column connections made using bolted end plates". *Bulletin of the New Zealand Society for Earthquake Engineering*, **15**(2): 82-92.

10 SCNZ (2007). "*Steel Connect*". Version 14.1 and 14.2, Steel Construction New Zealand. https://scnz.org/techincal-resources/connections-guide/

11 British Standards (1996). "*Eurocode 8: Design Provisions for Earthquake Resistance of Structures*". British Standards Institution London, UK.

12 ANSI/AISC-358 (2022). "*Prequalified Connections for Special and Intermediate Steel Moment Frames for Seismic Applications*". An American National Standard, American Institute of Steel Construction.

13 NZS3404 (1997). "*Steel Structures Standard: Part 1 & 2*". New Zealand Standards, Wellington.

14 Moroder D and Smith T (2020). "*Reinforcement of Timber Members*", Chapter 12.6 in *NZ Wood Design Guide*, Page 1-82. https://www.wpma.org.nz/timber-design-guides.html

15 ACI (2013). "*ACI 374.2R-13: Guide for Testing Reinforced Concrete Structural Elements under Slowly Applied Simulated Seismic Loads*". Technical Documents, ACI Committee 374.

16 Cowie K (2010). "*Research, Development and Design Rules of Moment Resisting Seismic Frames with Reduced Beam Sections*". SCNZ, NZ. https://scnz.org/research-development-and-design-rules-of-moment-resisting-seismic-frames-with-reduced-beam-sections/

17 Tombleson J, Newcombe M, Leslie S and Hewitt A (2024). "Standardised timber moment-resisting frames for multistorey buildings". *New Zealand Society for Earthquake Engineering Annual Conference*, 13pp.